



Biological and physical influences on soil ^{14}C seasonal dynamics in a temperate hardwood forest

C. L. Phillips^{1,*}, K. J. McFarlane¹, D. Risk², and A. R. Desai³

¹Center for Accelerator Mass Spectrometry, Lawrence Livermore National Laboratory, Livermore, CA, USA

²Department of Earth Sciences, St. Francis Xavier University, Antigonish, Nova Scotia, Canada

³Department of Atmospheric and Oceanic Sciences, University of Wisconsin, Madison, WI, USA

* now at: Department of Crops and Soil Science, Oregon State University, Corvallis, OR, USA

Correspondence to: C. L. Phillips (claire.phillips@oregonstate.edu)

Received: 4 June 2013 – Published in Biogeosciences Discuss.: 1 July 2013

Revised: 5 November 2013 – Accepted: 7 November 2013 – Published: 9 December 2013

Abstract. While radiocarbon (^{14}C) abundances in standing stocks of soil carbon have been used to evaluate rates of soil carbon turnover on timescales of several years to centuries, soil-respired $^{14}\text{CO}_2$ measurements are an important tool for identifying more immediate responses to disturbance and climate change. Soil $\Delta^{14}\text{CO}_2$ data, however, are often temporally sparse and could be interpreted better with more context for typical seasonal ranges and trends. We report on a semi-high-frequency sampling campaign to distinguish physical and biological drivers of soil $\Delta^{14}\text{CO}_2$ at a temperate forest site in northern Wisconsin, USA. We sampled $^{14}\text{CO}_2$ profiles every three weeks during snow-free months through 2012 in three intact plots and one trenched plot that excluded roots. Respired $\Delta^{14}\text{CO}_2$ declined through the summer in intact plots, shifting from an older C composition that contained more bomb ^{14}C to a younger composition more closely resembling present ^{14}C levels in the atmosphere. In the trenched plot, respired $\Delta^{14}\text{CO}_2$ was variable but remained comparatively higher than in intact plots, reflecting older bomb-enriched ^{14}C sources. Although respired $\Delta^{14}\text{CO}_2$ from intact plots correlated with soil moisture, related analyses did not support a clear cause-and-effect relationship with moisture. The initial decrease in $\Delta^{14}\text{CO}_2$ from spring to midsummer could be explained by increases in ^{14}C -deplete root respiration; however, $\Delta^{14}\text{CO}_2$ continued to decline in late summer after root activity decreased. We also investigated whether soil moisture impacted vertical partitioning of CO_2 production, but found this had little effect on respired $\Delta^{14}\text{CO}_2$ because CO_2 contained modern bomb C at depth, even in the trenched plot. This surprising result

contrasted with decades to centuries-old pre-bomb CO_2 produced in lab incubations of the same soils. Our results suggest that root-derived C and other recent C sources had dominant impacts on respired $\Delta^{14}\text{CO}_2$ in situ, even at depth. We propose that $\Delta^{14}\text{CO}_2$ may have declined through late summer in intact plots because of continued microbial turnover of root-derived C, following declines in root respiration. Our results agree with other studies showing declines in the ^{14}C content of soil respiration over the growing season, and suggest inputs of new photosynthates through roots are an important driver.

1 Introduction

The presence of large $\Delta^{14}\text{C}$ gradients in soil makes ^{14}C a potentially sensitive tool for detecting changes in respiration sources. The dynamic range of $\Delta^{14}\text{C}$ in putative respiratory substrates is often many times larger than for $\delta^{13}\text{C}$: deep soils generally contain an abundance of organic matter that is deplete in $\Delta^{14}\text{C}$ due to radioactive decay and the older age of deep carbon, while near-surface soils reflect litter additions containing “bomb C”, a legacy of aboveground thermonuclear weapons testing in the early 1960s (Gaudinski et al., 2000; Trumbore, 2000). Root and microbial respiration also often have different ^{14}C abundance, with root-derived CO_2 more closely resembling the recent atmosphere. This distinction has been employed to partition total soil respiration into heterotrophic (R_h) and autotrophic (R_a) components (Czimeczik et al., 2006; Hahn et al., 2006; Hicks Pries et al., 2013;

Schuur and Trumbore, 2006). While the distinctions between deep and shallow, and between R_h and R_a end-members are useful for partitioning, the large ^{14}C range in potential CO_2 sources may also accentuate seasonal and synoptic variability in soil $\Delta^{14}\text{CO}_2$. Although ^{14}C measurements have proven useful for identifying changes in respiratory sources following disturbance and climatic change (Czimczik et al., 2006; Hicks Pries et al., 2013; Hirsch et al., 2003; Schuur and Trumbore, 2006), our understanding of these effects could be improved with more information on $\Delta^{14}\text{CO}_2$ seasonal trends.

Several temporal studies have suggested that seasonal variation in soil-respired $\Delta^{14}\text{CO}_2$ may be large, and may therefore encode information about seasonal dynamics of respiratory sources. Gaudinski et al. (2000) found soil-respired $\Delta^{14}\text{CO}_2$ decreased by approximately 40‰ between May and December at Harvard Forest, a temperate deciduous system. Similarly, ecosystem-respired $\Delta^{14}\text{CO}_2$ at a tundra site in Alaska decreased over the summer by as much as 20‰ (Hicks Pries et al., 2013). Schuur and Trumbore (2006), however, found a large increase of 84‰ between June and August at a boreal forest site in Alaska. Unfortunately, temporal density in data sets with repeated sampling is generally very sparse, providing little information from which to fully describe seasonal variability or identify environmental drivers.

To help address this gap, in 2011–2012 we conducted a study of respired $\Delta^{14}\text{CO}_2$ dynamics at Willow Creek eddy covariance site, a temperate semi-deciduous forest in northern Wisconsin, USA. Our goal was to examine soil $\Delta^{14}\text{CO}_2$ dynamics through the growing season, and evaluate whether soil emissions also influenced atmospheric $\Delta^{14}\text{CO}_2$ dynamics. In this paper, we present our soil $\Delta^{14}\text{CO}_2$ observations and evaluate potential physical and biological processes underlying seasonal variation. Specifically, we evaluated impacts on soil $\Delta^{14}\text{CO}_2$ from the following processes:

1. Seasonal shifts in relative contributions of R_h and R_a .
2. Seasonal changes in relative contributions of deep and shallow CO_2 production.
3. Seasonal changes in $\Delta^{14}\text{C}$ of R_h , reflecting shifts in microbial substrates.

Although not an exhaustive list, by focusing on these processes we hoped to tease apart the relative influences of plant activity, microbial activity, and soil physical properties on respired $\Delta^{14}\text{CO}_2$ variability.

Investigating influences from these sources may help illuminate the utility and limitations of $\Delta^{14}\text{CO}_2$ for understanding soil metabolism. To our knowledge there has been no previous investigation of whether $\Delta^{14}\text{CO}_2$ of R_h varies seasonally, and R_h has been assumed to be isotopically static at seasonal to interannual timescales for partitioning heterotrophic and autotrophic respiration (Hicks Pries et al., 2013; Schuur and Trumbore, 2006) and for modeling rates of soil organic

matter turnover (Torn et al., 2002). If heterotrophic $\Delta^{14}\text{C}$ varies seasonally, this would indicate that the quality of soil C destabilized through time has greater environmental sensitivity than is presently represented by most soil biogeochemistry models. The effects of soil moisture and gas diffusion on respired $\Delta^{14}\text{CO}_2$ are also largely unexplored. Although soil moisture and gas diffusion can play roles in regulating deep versus shallow CO_2 production (Davidson et al., 2006; Phillips et al., 2012), gas diffusion is often neglected in favor of biological explanations for why sources of soil respiration vary through time. A simultaneous assessment of the relative influences on $^{14}\text{CO}_2$ by soil physical factors in addition to plant and microbial activity provides a check on existing assumptions and tendencies.

2 Methods

To evaluate influences of plant and microbial activity and soil physical factors, we measured surface CO_2 flux rates and subsurface profiles of CO_2 , $\Delta^{14}\text{CO}_2$, and $\delta^{13}\text{CO}_2$ in three intact soil plots and one plot that was trenched to exclude roots to 1 m depth. The trenched plot did not have spatial replication; therefore, a limitation of this study is that the treatments could not be statistically compared. Observations from the trenched plot, however, allowed us to examine in situ dynamics of microbially respired $\Delta^{14}\text{CO}_2$ through time, in the absence of live roots, which we compared with more common in vitro microbial respiration measurements from laboratory soil incubations. We used comparisons of the intact and trenched plots to estimate the relative contributions of R_h and R_a to total soil respiration. Subsurface profile measurements were used to estimate CO_2 and ^{14}C contributions from each soil horizon.

In addition, we employed a one-dimensional (1-D) soil CO_2 diffusive transport model to simulate how variations in the rate and isotopic composition of CO_2 production would be expected to impact $\Delta^{14}\text{CO}_2$ of soil air and surface flux. We used simulations as a second, independent approach for estimating $\Delta^{14}\text{CO}_2$ of microbial production from observations of soil air.

2.1 Site and soil description

The Willow Creek Ameriflux site is located in the Chequamegon National Forest of north central Wisconsin (45°48' W, 90°07' N), and is composed of mature, second growth hardwood trees approximately 80–100 yr old, dominated by sugar maple, basswood, and green ash (*Acer saccharum* Marshall, *Tilia Americana* L., *Fraxinus pennsylvanica* Marshall). Eddy covariance measurements have been made at the site since 1998, and plant and soil characteristics have been described in detail by others (Bolstad et al., 2004; Cook et al., 2004; Martin and Bolstad, 2005).

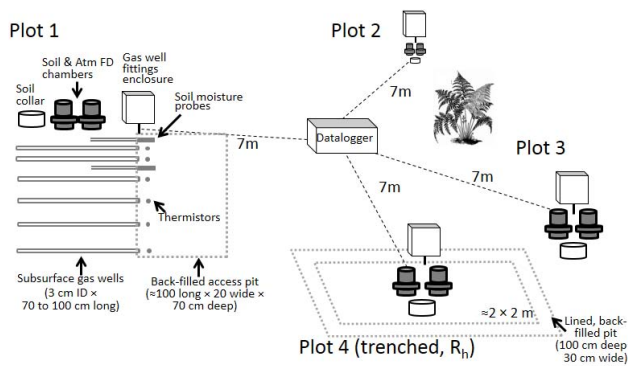


Fig. 1. Schematic of soil plot layout and below ground sensor installation.

In June 2011 we established a group of four soil plots centered about 30 m from the base of the eddy covariance tower (Fig. 1). In each plot we excavated a trench to 75 cm depth to characterize the profile and install instrumentation, removing soil in 10 cm increments to back-fill in the same order. Soils were deep and moderately permeable, formed from unsorted, coarse glacial till, and have evidence of mixing from windthrow, freeze-thaw, and earthworm activity. Texture in the four plots was classified as either sandy loams or loamy sands (mean texture in top 20 cm: 63 % sand, 31 % silt, 6 % clay, 5–12 % rock fragments). Soils lacked an O horizon, had an A horizon 8–12 cm in depth with a clear wavy boundary, followed by at least one B horizon, with variation among plots in iron depletions and accumulations, and finally a BC horizon starting at 50–60 cm with increased amounts of gravelly sand and gravel. We later found gas wells at and below 50 cm to be poorly drained until mid-summer.

We installed gas wells at 6 depths, at the interfaces between genetic horizons and several intermediate depths (nominal depths were 8, 15, 22, 30, 50, and 70 cm, with ≤ 3 cm variation across plots). We used a 2.5 cm diameter drill auger to create horizontal holes in the profile wall extending in 70–100 cm as permitted by stone content, and pounded gas wells into the holes. The wells were constructed of PVC pipe (70 to 100 cm long \times 3 cm ID; inner volume 0.5 to 0.7 L), which were perforated along the bottom with a row of 1 cm diameter holes to exchange air with the surrounding soil, and wrapped in Tyvek[®] polyethylene membrane to exclude water and soil macrofauna. Wells were staggered horizontally within a 15 cm range to reduce impacts on vertical CO_2 diffusion. Gas wells were capped at both ends, connected to the soil surface with two lengths of 1/8 polyethylene tubing, and the tubes were capped at the soil surface with plastic 2-way valves, which were housed in plastic enclosures. Thermistors were placed adjacent to each gas well to measure soil temperature (CS-107B, Campbell Scientific, Logan, Utah, USA), and TDR soil moisture probes were placed horizontally at 4 and 18 cm (CS-616, Campbell Scientific). Two sets of soil cores (5 cm diameter \times 5 cm long)

centered at 2.5, 7.5, 12.5, 18, 30, 40, and 60 cm were also removed from each exposed profile for isotopic analysis (see below), and for analysis of texture, porosity, and moisture release at the Oregon State University Soil Science Physical Characterization Lab.

To create the trenched plot, we dug a trench 30 cm wide \times 100 cm deep around all sides of a 2 m \times 2 m plot, and lined the trench with 0.13 mm thick polyethylene vapor barrier to prevent in-growth of new roots before refilling the trench with soil. Trenching was completed in early September 2011. The plot did not contain any woody plants, and emerging herbaceous plants (mostly grass) were clipped to their root crowns throughout 2012.

2.2 Soil CO_2 flux and profile air

Soil surface CO_2 flux was measured using forced diffusion (FD) chambers and Vaisala GMP343 CO_2 sensors (Vaisala Corp, Helsinki, Finland), as described by Risk et al. (2011). Each soil plot contained a FD soil chamber and atmospheric reference, and a co-located PVC soil collar for comparisons with the Licor-8100 soil flux system (Licor Environmental, Lincoln, NE, USA). FD CO_2 flux, temperature, and moisture were recorded hourly, and Licor CO_2 flux comparisons were made approximately every 3 weeks during the growing season.

Soil profile CO_2 was measured with the Licor-8100 IRGA, by first circulating air through a soda-lime trap to remove CO_2 from the Licor internal volume and tubing, and then switching valves to shut off the CO_2 trap and circulate soil air between the gas well and Licor. Soil air was circulated in a closed loop for several minutes until concentrations stabilized. A 1 μm air filter and a 50 mL canister of Drierite[™] plumbed to the Licor inlet trapped particles and moisture from incoming soil air. The gas well tubing was also pre-purged by removing and discarding 50 mL of air with a syringe before connecting the tubing to the Licor.

After measuring CO_2 , we sampled soil air for isotopic analysis using pre-evacuated 400 mL stainless steel canisters (Restek Corp #24188, PA, USA) or activated molecular sieve traps (Gaudinski et al., 2000). To prepare canisters, we pre-cleaned them with N_2 and heat following the manufacturer's instructions, evacuated them to ≤ 1 mTorr, and capped the valves with rubber septa prior to overnight shipping to the field site. In the field, we connected a syringe needle to the gas well tubing and filled the canisters by piercing the septa. To sample with molecular sieve traps, we used the Licor to pull soil air through the trap in a flow-through configuration. During trapping, we maintained a flow rate of 60 mL min^{-1} , and timed trapping to collect 2 mg C (total trapping time ranged 30 s to 15 min, depending on concentration). The molecular sieve (13X 8/12 beads, Grace) was washed, and then pre-conditioned by baking at 750 $^\circ\text{C}$ under vacuum for 12 h. Molecular sieve traps were activated using the same procedure for extraction, below.

Atmospheric samples from the eddy covariance tower were also sampled from just above the forest canopy at 21 m above ground level into glass flasks, using a programmable flask package and compressor (Andrews et al., 2013). These whole-air samples were collected approximately every 6 days at 12:30 a.m. local time, so that they reflected respiration not influenced by photosynthesis.

2.3 Root and soil incubations

We collected roots from 0–5 cm in three locations in August 2011 to determine the $\Delta^{14}\text{C}$ of R_a . In the field, roots were rinsed in distilled water and placed in sterilized Mason jars. Atmospheric CO_2 was removed from the jar headspace by recirculating air through a soda lime trap and IRGA. The jars were shipped overnight to the Center for Accelerator Mass Spectrometry (CAMS) at Lawrence Livermore National Laboratory, and CO_2 was extracted within 48 h, as described below.

Soils were incubated to compare laboratory measurements of R_h with observations from the trenched plot. Soil cores were sampled from each plot during well installation, and shipped on ice to CAMS. We removed the majority of roots by hand-picking, and allowed the remainder to senesce by resting the soils for two weeks before sealing the incubation jars. The closed jars were purged with CO_2 -free air, and incubated at 25 °C until at least 0.5 mg C- CO_2 could be extracted from the headspace. Incubation time ranged from 4 to 126 days, depending on the activity of each sample.

2.4 ^{14}C sample processing

CO_2 from canisters, flasks, and incubation jars was purified cryogenically at CAMS using a vacuum line, and CO_2 trapped on molecular sieves was released by baking at 650 °C under vacuum for 30 min while condensing CO_2 cryogenically. Purified CO_2 was reduced to graphite on iron powder in the presence of H_2 (Vogel et al., 1984). Subsamples of CO_2 were analyzed for $\delta^{13}\text{C}$ at the UC Davis Stable Isotope Laboratory (GVI Optima Stable Isotope Ratio Mass Spectrometer), and were used to correct ^{14}C values for mass-dependent fractionation.

Radiocarbon abundance in graphitized samples was measured on the Van de Graff FN Accelerator Mass Spectrometer (AMS) at CAMS, is reported in $\Delta^{14}\text{C}$ notation with a correction for ^{14}C decay since 1950 (Stuiver and Polach, 1977). In $\Delta^{14}\text{C}$ notation, values > 0 ‰ indicate the presence of “bomb” C that was fixed after 1950, whereas values ≤ 0 ‰ indicate C that was fixed prior to 1950. AMS samples had an average precision of 2.5 ‰. Total uncertainty associated with AMS plus sampling and CO_2 extraction was estimated to be 8.7 ‰ for molecular sieve traps, and 3.2 ‰ for air canisters, based on the standard deviation of contemporary atmosphere process standards ($N = 5$ for each sample type).

2.5 Data analysis

The analysis of field data had three components: (1) calculating $^{14}\text{CO}_2$ of surface flux from profile measurements, (2) estimating CO_2 and ^{14}C production by soil horizon, and (3) partitioning total soil respiration into R_h and R_a . Each component is discussed below.

2.5.1 Surface flux $^{14}\text{CO}_2$

Due to recent reports of isotopic disequilibria caused by surface chambers (Albanito et al., 2012; Midwood and Millard, 2011; Nickerson and Risk, 2009a), for this study we focused on profile measurements, which may be less prone to sampling artifacts. We estimated $\Delta^{14}\text{C}$ of surface flux from profile measurements using a gradient approach following Nickerson et al. (2013). The gradient approach is often used to calculate surface CO_2 flux from subsurface concentrations by applying Fick’s first law of diffusion:

$$F = D(z) \frac{dC}{dz}, \quad (1)$$

where F is the CO_2 flux density ($\mu\text{mol m}^{-2} \text{s}^{-1}$), $D(z)$ is the soil CO_2 diffusivity ($\text{m}^2 \text{s}^{-1}$) at depth z (m), and C is the CO_2 concentration ($\mu\text{mol m}^{-3}$). As described by Nickerson et al. (2013), if we assume the isotopologues of CO_2 ($^{12}\text{CO}_2$, $^{13}\text{CO}_2$, and $^{14}\text{CO}_2$) diffuse independently of one another, we can use Eq. (1) to model fluxes of each. The isotopic ratio of ^{14}C to ^{12}C in surface flux can thus be modeled as the quotient of Eq. (1) applied to $^{14}\text{CO}_2$ and $^{12}\text{CO}_2$:

$$\left[\frac{^{14}\text{C}}{^{12}\text{C}} \right]_F = \frac{F^{14}}{F^{12}} = \frac{D^{14}(z) \frac{d^{14}\text{C}}{dz}}{D^{12}(z) \frac{d^{12}\text{C}}{dz}}, \quad (2)$$

where F^{14} and F^{12} are the fluxes of $^{14}\text{CO}_2$ and $^{12}\text{CO}_2$, respectively, and $D^{14}(z)$ and $D^{12}(z)$ are the depth-specific diffusivities for each isotopologue. The quotient of diffusion coefficients for a rare and common isotope is also the inverse of the fractionation factor, α , which is 1.0044 for $^{13}\text{CO}_2$ diffusion through soil (Cerling et al., 1991), and is estimated to be approximately 1.0088 for $^{14}\text{CO}_2$ (Southon, 2011). Using this relationship, we can simplify and discretize Eq. (2) to yield:

$$\left[\frac{^{14}\text{C}}{^{12}\text{C}} \right]_F = \frac{1}{\alpha^{14}} \left[\frac{C_{z_2}^{14} - C_{z_1}^{14}}{C_{z_2}^{12} - C_{z_1}^{12}} \right], \quad (3)$$

where α^{14} is the fractionation factor for ^{14}C , and z_1 and z_2 are arbitrary depths with increasing CO_2 concentration. Similarly, the $^{13}\text{C}/^{12}\text{C}$ ratio in surface flux can be calculated by replacing ^{14}C with ^{13}C values. Note that Eq. (4) indicates the isotopic ratio of surface flux can be calculated without knowing the diffusivity of CO_2 in soil which is difficult to measure well and uncertain to model (Pinging et al., 2010).

To convert between Δ values (for reporting purposes) and absolute $^{14}\text{C}/^{12}\text{C}$ ratios (for flux calculations), we used the

following equations:

$$\Delta = (\text{FM} \cdot e^{\frac{1950-\text{Yr}}{8267}} - 1) \times 1000, \quad (4)$$

where Δ notation (‰) is calculated by standardizing fraction modern (FM) to the year 1950 to allow inter-comparison of samples from different analysis years (Yr), and 8267 yr is the ¹⁴C mean decay rate. FM was related to the sample ¹⁴C/¹²C ratio following the derivation in Southon et al. (2011), where it is shown that ¹⁴C activity \approx ¹⁴C/¹²C.

$$\text{FM} = \frac{\frac{\left[\frac{^{14}\text{C}}{^{12}\text{C}}\right]_S}{0.95 \cdot \left[\frac{^{14}\text{C}}{^{12}\text{C}}\right]_{\text{OXI}}} \left(1 - \frac{25}{1000}\right)^2}{\left(1 + \frac{\delta^{13}\text{C}}{1000}\right)^2}} \quad (5)$$

In the equation above $\left[\frac{^{14}\text{C}}{^{12}\text{C}}\right]_S$ is the sample ¹⁴C ratio, $\delta^{13}\text{C}$ is the sample ¹³C abundance in ‰ notation, which is used to normalize the ¹⁴C ratio for mass-based fractionation to $\delta^{13}\text{C} = -25$ ‰, and $0.95 \cdot \left[\frac{^{14}\text{C}}{^{12}\text{C}}\right]_{\text{OXI}}$ is the normalized ¹⁴C ratio of the oxalic acid I standard.

We calculated the ¹³C and ¹⁴C composition of surface fluxes at Willow Creek using Eq. (3) with data from the soil surface ($z_1 = 0$ cm) and the shallowest gas wells ($z_2 = 7$ or 8 cm). On two sampling dates, however, there were missing observations in plot 4 at the 7 cm depth, and we instead used data from gas wells at 14 cm. To assess errors from this gap-filling approach, we compared flux calculations for days when both the shallowest well and next depth were available ($N = 28$) and found the gap-filling approach caused a small positive bias in estimated surface flux (mean difference in $\Delta^{14}\text{CO}_2 = 2.5$ ‰, $\sigma = 7.3$ ‰), which was similar in magnitude to the combined AMS and sampling error. Observations for the soil surface were only available for about half the sampling dates; for missing dates we assumed $\delta^{13}\text{C} = -9.5 \pm 1$ ‰ and $\Delta^{14}\text{C} = 30 \pm 5$ ‰, based on an average of available data. To estimate uncertainty for surface flux isotopic ratios, we applied Monte Carlo simulations (1000 iterations) to propagate the uncertainty associated with each measurement in Eq. (3).

2.5.2 CO₂ and ¹⁴CO₂ production by soil horizon

To vertically partition the production of CO₂, we again applied Fick's law (Eq. 1) to determine fluxes from subsurface soil layers. After experimenting and finding no functional types that satisfactorily fit the CO₂ profiles through time, we chose to calculate dC/dz across soil layers by discrete difference. We used the following discretized form of Fick's law:

$$F(z_1) = \bar{D}(z_1, z_2) \left[\frac{C_{z_2} - C_{z_1}}{z_2 - z_1} \right], \quad (6)$$

where $F(z_1)$ is the flux at the top of a soil layer, $\bar{D}(z_1, z_2)$ is the average diffusivity within the layer (following Turcu

et al., 2005), and C_{z_1} and C_{z_2} are CO₂ concentrations in gas wells at the top and bottom of the soil layer. We modeled soil diffusivity following Moldrup et al. (2004) based on soil water content, porosity, and moisture release characteristics. Because the four soil plots had similar vertical profiles for physical variables, we compiled porosity and moisture release data from all plots and applied a loess fit to interpolate between measured depths. Diffusivity was modeled with soil moisture data specific to each plot, and moisture between measured depths was estimated by linear interpolation. Diffusivity was corrected using soil temperature measurements from each plot, as in Pingintha et al. (2010). Good agreement between surface flux rates calculated with Eq. (7) and direct measurements with the Licor 8100 supported the accuracy of this approach (Slope = 0.95, $R^2 = 0.89$, $N = 46$).

The production of CO₂ in each soil layer was estimated as the difference between fluxes entering the bottom and leaving the top of the layer (Davidson et al., 2006; Gaudinski et al., 2000), as follows:

$$P(z_1, z_2) = F(z_1) - F(z_2), \quad (7)$$

where $P(z_1, z_2)$ is the production in the soil layer between depths z_1 and z_2 . The $\Delta^{14}\text{C}$ of production in each layer was calculated as in Gaudinski et al. (2000).

$$\Delta P(z_1, z_2) = \frac{(F(z_2) + P(z_1, z_2)) \cdot \Delta F(z_1) - F(z_2) \cdot \Delta F(z_2)}{P(z_1, z_2)} \quad (8)$$

where Δ indicates $\Delta^{14}\text{C}$ of production and flux in ‰ units. Uncertainty of production rates and isotopic composition were estimated with Monte Carlo simulations, randomly sampling errors to add to each component measurement within its range of analytical uncertainty, for 1000 iterations.

2.5.3 Contributions of R_h and R_a

Although trenched plots have several known limitations for estimating heterotrophic soil activity (e.g., increased soil moisture, root senescence, and potential changes in microbial composition), we used comparisons of the trenched and intact plots to partition total soil respiration (R_{tot}) by two methods: bulk surface fluxes, and isotopic mixing. We compared both these approaches, first computing R_h/R_{tot} as the quotient of surface CO₂ flux from the trenched plot and the average of the intact plots, and second by applying a two-end-member isotopic mixing equation:

$$\frac{R_h}{R_{\text{tot}}} = \frac{\Delta R_{\text{tot}} - \Delta R_a}{\Delta R_h - \Delta R_a}, \quad (9)$$

where ΔR_h and ΔR_{tot} are the $\Delta^{14}\text{C}$ of surface flux from trenched plot and intact plots, respectively, and ΔR_a was estimated from root incubations. Uncertainty associated with isotopic partitioning estimates was calculated following Phillips and Gregg (2001).

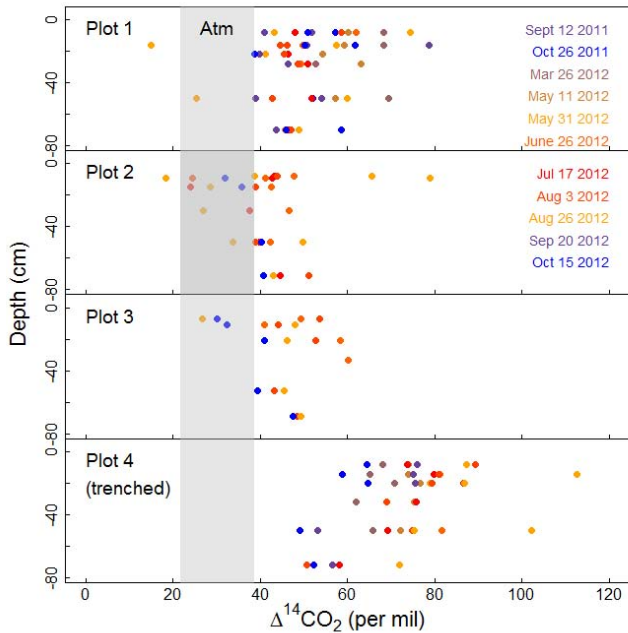


Fig. 2. Soil air $^{14}\text{CO}_2$ for intact and trenched plots. Grey bar shows range of atmospheric $^{14}\text{CO}_2$. Error bars not shown for clarity, uncertainty for $\Delta^{14}\text{CO}_2$ measurements ranged approximately 2–9‰ (see methods).

2.6 Diffusional model simulations

We adopted the model described in Nickerson and Risk (2009b) to simulate diffusion of $^{14}\text{CO}_2$ in addition to other isotopologues. Our modeled soil profile was 1 m deep with 100 layers, and at each time step gas transport between neighboring layers was calculated with a 1-D discrete version of Fick's law, using isotopologue-specific diffusivities. Diffusivity of $^{12}\text{CO}_2$ was calculated from soil physical variables following Moldrup et al. (2004), and the diffusivity of $^{13}\text{CO}_2$ and $^{14}\text{CO}_2$ were calculated by multiplying the Moldrup diffusivity by fractionation factors of 1.0044 and 1.0088, respectively. For all simulations we initialized the CO_2 concentration profile with an analytical steady-state solution (Nickerson and Risk, 2009b). We iterated the model with a 1 s time step until the concentration and isotopic composition of soil profiles were stable for at least 3 model days. The default soil physical and biological variables reflect values observed at Willow Creek, and are shown in Table 1.

3 Results

3.1 General patterns

The $\Delta^{14}\text{CO}_2$ of soil air in intact profiles was intermediate between the atmosphere and the trenched plot profile (Fig. 2), with $\Delta^{14}\text{CO}_2$ in intact profiles averaging 48‰ (S.D. = 9‰, $N = 85$), trenched plot observations averaging

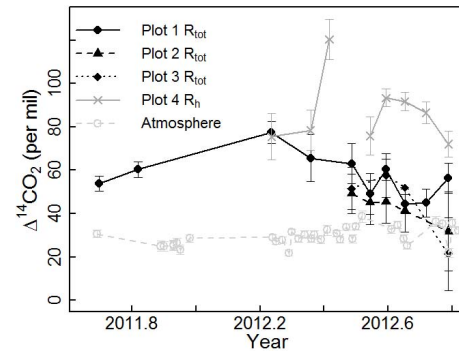


Fig. 3. Computed $\Delta^{14}\text{CO}_2$ of surface flux (R_{tot} for intact plots and R_{h} for trenched plot) and atmospheric $\Delta^{14}\text{CO}_2$ (21 m above ground level) for the same period. Note that for the trenched plot, fluxes on 2012.42 and 2012.49 were calculated using measurements from 14 cm depth rather than 7 cm, due to missing data.

73‰ (S.D. = 13‰, $N = 41$), and atmospheric samples from the tower averaging 29‰ (S.D. = 4‰, $N = 41$, see also Fig. 3). The total range in soil $^{14}\text{CO}_2$ over the sampling period was about two to three times greater than in air samples from the tower, indicating atmospheric variation was not the primary factor driving soil $^{14}\text{CO}_2$ variability.

The computed $\Delta^{14}\text{CO}_2$ of surface fluxes (Fig. 3) indicated microbial soil respiration was more enriched in ^{14}C than total respiration by a seasonal average of 34‰ (95% CI = 23–44‰). This is approximately equivalent to a mean age six to eight years older, based on the recent rate of decline of atmospheric bomb ^{14}C of 4 to 5.5‰ yr^{-1} (Graven et al., 2012). In intact plots, respired $\Delta^{14}\text{C}$ decreased over the course of the 2012 growing season, from a high value in March of 77‰ (only Plot 1 sampled) to a low in October of 37‰ (Plots 1–3, averaged). This 40‰ seasonal decrease was also significantly correlated with soil moisture (Fig. 4). In contrast to the intact plots, microbially respired $\Delta^{14}\text{C}$ from the trenched plot remained comparatively elevated through the growing season.

Other impacts of trenching included a substantial decrease in surface CO_2 flux, by an average of 39% over the course of the 2012 growing season (Fig. 5a), and elevated summer soil moisture compared to the intact plots (Fig. 5c). The decrease in CO_2 flux rate and the lack of soil drying, which was likely due to cessation of plant transpiration, both provided strong indications that trenching was successful at excising live roots. We observed no impacts of trenching on soil temperature (Fig. 5b).

Surface CO_2 flux measurements using the novel FD chambers compared favorably with periodic side-by-side LI-8100 measurements, producing highly linear relationships (overall $R^2 = 0.6$). FD chambers tended to measure lower fluxes than the LI-8100, however, in contrast to earlier laboratory comparisons (Risk et al., 2011). While it is difficult to know under field conditions which instrument is most correct, we

Table 1. Default parameters in model simulations.

Parameter	Default value	Default source
Soil porosity (v/v)	gradient, 0.65 to 0.34	soil cores
Water content (v/v)	0.27	growing season mean at 18 cm, plot 4
CO_2 production rate ($\mu\text{mol m}^{-2} \text{s}^{-1}$)	2.71	growing season mean, plot 4
CO_2 production vertical distribution	gradient, 97 % in 0–20 cm	laboratory incubations
$\Delta^{14}\text{C}$ production (‰)	gradient, 82 to –198‰	laboratory incubations
$\delta^{13}\text{C}$ production (‰ PDB)	gradient, –28‰ to –17‰	laboratory incubations
Atmosphere CO_2 (ppm)	385	tower
Atmosphere $\Delta^{14}\text{C}$ (‰)	29‰	tower
Atmosphere $\delta^{13}\text{C}$ (‰ PDB)	–9.5‰	tower

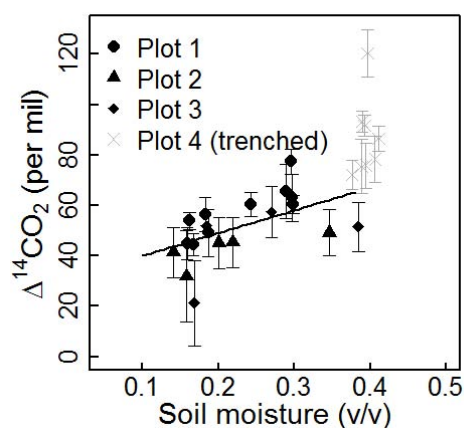


Fig. 4. Surface flux $\Delta^{14}\text{CO}_2$ versus soil moisture. In intact soil plots $\Delta^{14}\text{CO}_2$ and moisture were significantly correlated (slope $p=0.01$, $R^2=0.31$). With the trenched plot included, slope $p<0.001$, $R^2=0.62$.

chose to normalize all the FD chambers to the common LI-8100 instrument, by adjusting each FD using a linear multiplier and offset obtained from side-by-side measurements made on >20 different days. The corrected fluxes are presented here (Fig. 5). FD measurements also had a considerable number of high magnitude fluxes, or spikes, which have also been noted in FD measurements in other field studies (Lavoie et al., 2012; Risk et al., 2013). No attempts were made to smooth the soil flux data, because the spikes may be natural high-frequency phenomena (i.e., pressure pumping) that are not normally detected by the comparatively slow-sampling, dynamic soil chambers like the LI-8100 system. Alternatively, the spikes may be due to sampling error, due to transient deviations between the FD's two internal CO_2 sensors that simultaneously measure soil and atmospheric concentrations.

Isotopically, microbially respired fluxes from the trenched plot did not have identifiable seasonal trends, but they had similar total variation to fluxes from the intact plots. For most days surface fluxes from the trenched plot fell within a 20 %

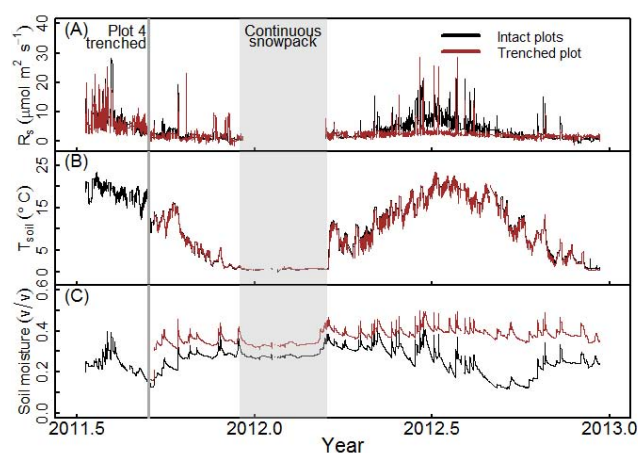


Fig. 5. Time series of (a) soil CO_2 flux measured with forced-diffusion probes, (b) soil temperature at 5 cm, and (c) volumetric soil moisture at 4 cm. The mean of the three intact plots is shown for clarity.

range for $\Delta^{14}\text{CO}_2$, but one observation exceeded the minimum by almost 50 %. It is important to note, however, that this high value was calculated using the 14 cm gas well depth to gap-fill missing data from the 7 cm depth, which may have induced a positive bias in calculated surface flux $\Delta^{14}\text{CO}_2$. On the other hand, the 14 cm depth was not uniquely elevated in ^{14}C on that particular sampling day. High $\Delta^{14}\text{CO}_2$ levels exceeding 100 ‰ were found in both shallow and deep gas wells from this profile (Fig. 2, bottom panel).

3.2 Explanation 1: changing R_h and R_a contributions

To account for seasonal declines in respired $^{14}\text{CO}_2$ from the intact plots, we first examined changes in relative contributions from heterotrophic and autotrophic CO_2 sources. We expected that increasing contributions from ^{14}C -deplete root respiration could lead to decreases in total soil respired $^{14}\text{CO}_2$. Root-respired $^{14}\text{CO}_2$ measured from incubations of roots from 0–5 cm depth was 39 ‰ (S.D. = 4 ‰, $N=4$).

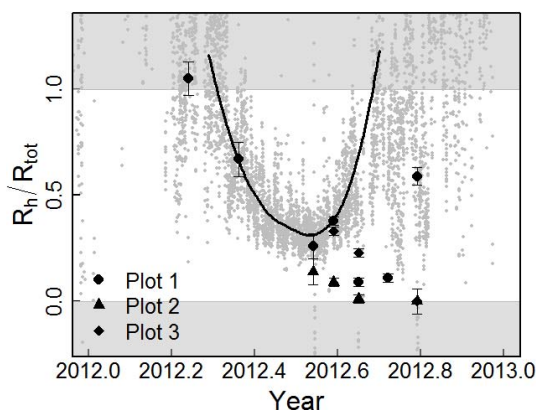


Fig. 6. Heterotrophic contributions to total soil respiration, estimated by two methods. Grey points show hourly R_h/R_{tot} estimated from the quotient of surface fluxes from the trenched and intact plots (all intact plots averaged). Solid black line shows mean quotient estimated by loess fitting. Black points show ^{14}C partitioning estimates for each plot.

Consistent with expectation, root-respired CO_2 had less ^{14}C than microbially respired (i.e., surface flux from the trenched plot), with a seasonally averaged difference of 46‰ (95% CI = 33–60‰). In terms of C age, CO_2 respired from the trenched plot was 8 to 12 yr older than root respiration.

We estimated contributions from heterotrophic and autotrophic sources by two methods. Our first approach was to compare the quotient of surface CO_2 fluxes from the intact and trenched plots. This approach produced a U-shaped seasonal pattern for R_h/R_{tot} (Fig. 6). Heterotrophic contributions descended from 100% in March to a minimum of about 30% in mid-summer, and returned to 100% by mid-October. Note that the quotient of surface fluxes often exceeded 1 outside the growing season because rates in the trenched and intact plots were similar to each other and near zero.

Estimates of R_h/R_{tot} using the second approach, an isotopic mixing equation, provided similar estimates as surface fluxes from March through July, but then diverged and remained close to zero through the remainder of the growing season. Two $\Delta^{14}\text{C}$ measurements from the intact plots were actually more deplete in ^{14}C than the autotrophic end-member, providing negative estimates of R_h contributions, and these are shown on the zero line in Fig. 6. Essentially, the two partitioning approaches diverged because flux rates in the intact plots returned to levels similar to the trenched plot by the end of the growing season, but $\Delta^{14}\text{C}$ did not. Both partitioning approaches pointed towards decreasing heterotrophic contributions in the first half of the summer as a possible explanation for the decrease in respired $^{14}\text{CO}_2$ from intact plots, but other mechanisms are needed to explain the continued $\Delta^{14}\text{C}$ decrease in late summer.

3.3 Explanation 2: changing vertical CO_2 contributions

We next investigated whether the seasonal decline in respired $^{14}\text{CO}_2$ from intact plots was related to changes in the vertical distribution of CO_2 production in the soil profile. Because deep soil carbon is older and has less ^{14}C than shallow substrates, we expected seasonal warming and drying of the soil profile could cause deep C to become destabilized and respired. We found, however, only weak evidence that variation in the vertical distribution of CO_2 production influenced the ^{14}C signature of surface respiration.

Vertical partitioning calculations indicated approximately 40 to 80% of total production originated from the uppermost 8 cm (Fig. 7). The $\Delta^{14}\text{C}$ of surface flux tended to increase with the fraction of CO_2 produced in the uppermost soil layer (slope $p = 0.002$, $R^2 = 0.3$), but the relationship was only significant when all four plots were analyzed. When the trenched plot was excluded, the slope of this relationship had a p value of 0.07.

Vertical partitioning exhibited some seasonality (Fig. 7a), and we found a weak correlation between the fraction of CO_2 produced by the top layer and soil moisture, but only when all four plots were analyzed (slope $p = 0.01$, $R^2 = 0.12$). Furthermore, in contrast to our expectation of deep CO_2 containing less ^{14}C , we found the $\Delta^{14}\text{C}$ of soil air did not show consistent patterns with depth (Fig. 2). Gradients were especially variable in the intact soil plots, sometimes increasing with depth and sometimes decreasing. To investigate vertical CO_2 gradients in more detail, we also calculated the $\Delta^{14}\text{C}$ of CO_2 produced in each subsurface horizon (Fig. 8), in contrast to examining only the $^{14}\text{CO}_2$ gradients in soil air, which are attenuated by diffusion. Unfortunately, we found that $\Delta^{14}\text{C}$ production estimates were prone to error in deep soil where bulk CO_2 production rates were low, because the bulk production term occurs in the denominator of $\Delta^{14}\text{C}$ calculations and tends to inflate isotopic errors in the numerator (Eqs. 8 and 9). We therefore present only a subset of the calculated production $\Delta^{14}\text{C}$ results, filtering out values where production rate was $\leq 0.2 \mu\text{mol m}^{-2} \text{s}^{-1}$ for the soil layer. The remaining observations, where we were focused between 0 and 20 cm, indicated no vertical trends in $\Delta^{14}\text{C}$ of production. The lack of vertical gradient in $\Delta^{14}\text{C}$ of CO_2 production may also indicate that CO_2 in this layer is root derived. In contrast to soil organic matter, roots have limited age gradients with soil depth (Schrumpp et al., 2013).

From the vertical partitioning analysis, we did not find a compelling explanation for the correlation between respired $^{14}\text{CO}_2$ and moisture. Although the vertical distribution of CO_2 production varied substantially through time, correlations with soil moisture and ^{14}C were weak, and we lacked evidence that $^{14}\text{CO}_2$ abundance decreases with depth.

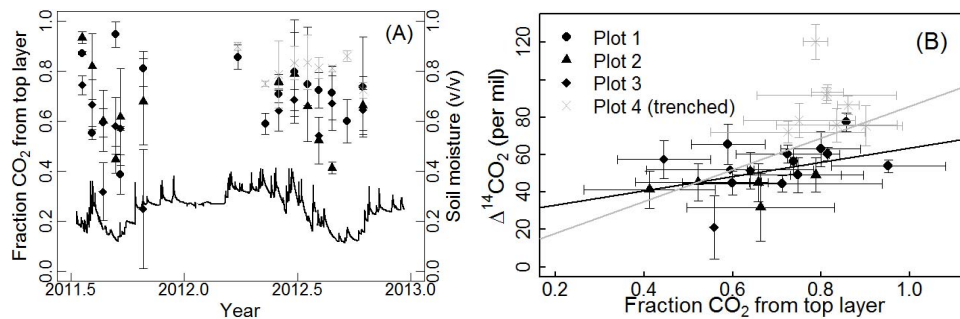


Fig. 7. Vertical partitioning, expressed as fraction of CO_2 produced in uppermost soil layer (top 7 to 8 cm). Errors bars were calculated from Monte Carlo simulations to propagate uncertainties from gas well measurements. **(A)** variation in vertical partitioning through time, with soil water content shown for seasonal context, and **(B)** vertical partitioning versus $\Delta^{14}\text{C}$ of surface flux. The grey regression line includes plot 4 (slope $p < 0.01$, $R^2 = 0.29$) and the black regression line excludes plot 4 (slope $p = 0.07$, $R^2 = 0.19$).

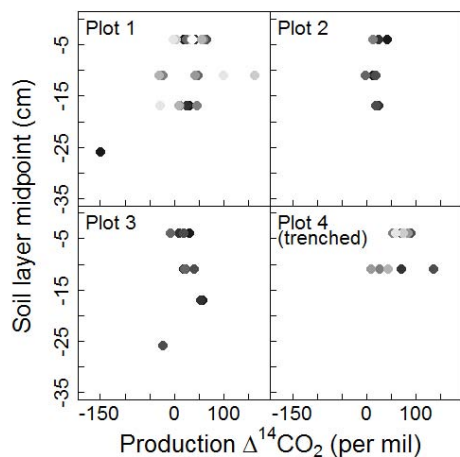


Fig. 8. Variation in estimated $\Delta^{14}\text{CO}_2$ production profiles over the sampling period. Sampling days are distinguished by shade, from dark (late 2011 and early 2012) to light (late 2012). Because estimated errors are inflated by low production rates (see Eq. 9), we omitted $\sim 20\%$ of observations where soil layer CO_2 production rate was $\leq 0.2 \mu\text{mol m}^{-2} \text{s}^{-1}$.

3.4 Explanation 3: changes in $\Delta^{14}\text{C}$ of heterotrophic respiration

As stated in the general trends, surface fluxes from the trenched plot varied in $\Delta^{14}\text{C}$ by as much as 50‰ through the 2012 growing season, but remained comparatively high and did not seem to explain the decrease in respired $^{14}\text{CO}_2$ from intact plots. Observations from the trenched plot provided a unique opportunity to examine R_h in a more dynamic environment than traditional laboratory incubations. To place these trenched plot results in context, here we compare the trenched plot observations, which are essentially an in situ incubation, to more commonplace in vitro incubations in static laboratory conditions.

We found that for both laboratory incubations and trenched plot measurements, the vertical distribution of soil

CO_2 production was similar (Fig. 9b). Both approaches had the highest production rates between 0–20 cm, and very little production in deeper soil. This similarity conferred some confidence that manipulating the soil either by trenching or by more disruptive coring did not alter the relative microbial activity of deep versus shallow soil. We found striking differences, however, between $^{14}\text{CO}_2$ produced in laboratory incubations and $^{14}\text{CO}_2$ in the trenched plot (Fig. 9a). In laboratory incubations, respired $^{14}\text{CO}_2$ had a similar vertical gradient as bulk solid soil. Below 15 cm, CO_2 from incubations did not contain bomb C (i.e., $\Delta^{14}\text{C} < 0\text{‰}$) and reflected the old C substrates present in deep soil. In contrast, CO_2 in the trenched plot was greater than 0‰ at all depths, containing bomb C throughout the profile. Although in situ soil air is somewhat impacted by atmospheric CO_2 invasion, atmospheric effects were unlikely to have substantial impact, because soil CO_2 concentrations ranged five to 20 times greater than atmospheric CO_2 . Following the same incubation procedure used by many others (Cisneros-Dozal et al., 2006; Gaudinski et al., 2000; Schuur and Trumbore, 2006), we picked out the majority of roots from soil cores before incubating them, and this root removal may have dramatically altered respired $^{14}\text{CO}_2$ in comparison to the trenched plot. This comparison between in vitro and in situ microbial respiration suggests that C substrates for respiration are very different in lab incubations from the field, particularly below 15 cm. In the field, C from decaying roots was an important microbial substrate in the trenched plot, throughout the profile. The $\Delta^{14}\text{C}$ of microbial respiration from the trenched plot was influenced not only by the quantity and quality of soil organic matter pools, but perhaps more importantly by the availability of root C. In the lab incubations release of old C due to disturbance of ped structure may have augmented release of old C, as in Ewing et al. (2006).

3.5 Dynamic simulations

Because incubation $^{14}\text{CO}_2$ measurements are used in many studies to assess the age of C that is actively utilized by

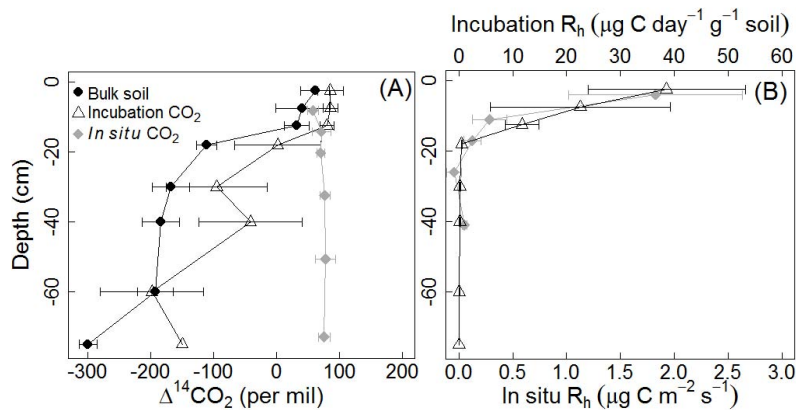


Fig. 9. (a) $\Delta^{14}\text{C}$ of bulk solid soil, CO_2 respired in laboratory incubations, and soil air CO_2 from trenched plot (note the respiration units differ for field and laboratory samples). (b) CO_2 production rate in incubations and in trenched plot. Error bars for bulk soil and laboratory incubations are the standard deviation of replicate cores ($N = 3$), and for the trenched plot are the standard deviation of sampling dates ($N = 10$).

microbes, and to characterize heterotrophic end-members for respiration source partitioning, we wanted to confirm the apparent discrepancy between field and laboratory microbial $^{14}\text{CO}_2$ production. We used a dynamic CO_2 diffusion model as an alternate tool to constrain the $\Delta^{14}\text{C}$ of production in the trenched plot. We prescribed a range of production $\Delta^{14}\text{C}$ profiles to assess if microbial production of old ^{14}C -deplete CO_2 at depth could give rise to modern soil air CO_2 gradients (i.e., $\Delta^{14}\text{C} > 0\text{‰}$), like we observed in the trenched plot. For these simulations we assumed that the vertical distribution of bulk CO_2 production was the same as observed in the incubations, and we parameterized all other soil variables to match actual soil conditions as much as possible (Table 1). For the first simulation (Fig. 10a), we started with $^{14}\text{CO}_2$ production profiles that were observed in the laboratory incubations. With each subsequent simulation we included more ^{14}C at depth, progressing towards a vertically constant isotopic profile with $\Delta^{14}\text{C}$ production = 86‰ (the $\Delta^{14}\text{C}$ produced by the 0–5 cm depth incubation). In other words, if microbial production in the trenched plot had the same ^{14}C abundance as in lab incubations, we would expect steady-state soil CO_2 in the trenched plot to look similar to the black line in Fig. 10a. This set of simulations demonstrated two important points. First, it highlighted that the $\Delta^{14}\text{C}$ soil air CO_2 profiles differ somewhat from $\Delta^{14}\text{C}$ CO_2 production profiles, due to diffusive mixing and infiltration of atmospheric CO_2 . Second, it showed that the $\Delta^{14}\text{C}$ produced in lab incubations was much too old in deep soil to give rise to the CO_2 profiles observed in the trenched plot. In order to obtain $^{14}\text{CO}_2$ soil air profiles in the range we observed in the trenched plot (50–120‰), the $\Delta^{14}\text{C}$ of production would have to exceed 0‰ through the length of a 1 m profile (as in Fig. 10e or f).

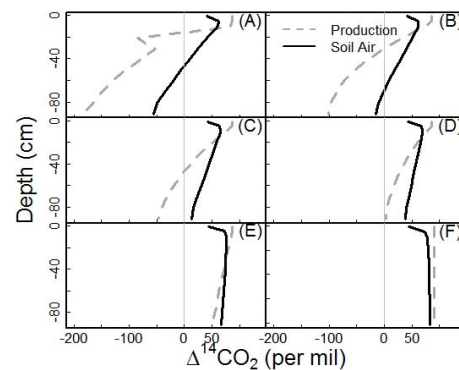


Fig. 10. Comparison of production and soil air $^{14}\text{CO}_2$ profiles from dynamic simulations of 1-D diffusion.

4 Discussion

4.1 Influences on $^{14}\text{CO}_2$ seasonal variation

We found a monotonic decrease in $\Delta^{14}\text{C}$ of surface flux from intact plots through the 2012 growing season, which was consistent with the seasonal decline found by Gaudinski et al. (2000) at Harvard Forest, and the decline in ecosystem-respired $^{14}\text{CO}_2$ at an Alaska tundra site by Hicks Pries et al. (2013). We examined three possible explanations for this seasonal decline: shifts in autotrophic versus heterotrophic contributions, deep versus shallow contributions, and variability in $\Delta^{14}\text{C}$ of heterotrophic respiration. We found substantial seasonal variation in all of these potential explanatory variables, but each had a weak or no relationship with respired $^{14}\text{CO}_2$. Although our trenched plot treatment was not spatially replicated, the $\Delta^{14}\text{C}$ of respiration from the trenched plot was consistently greater than intact plots following the first spring sampling event. Based on this shift in respired CO_2 towards older, ^{14}C -enriched bomb C when

roots were cutoff, as well as the shift in microbial respiration towards even older pre-bomb C when roots were picked out from incubated soils, we believe one of the more compelling explanations for the growing-season decline in respired $^{14}\text{CO}_2$ was an increasing dependence through the summer on newly photosynthesized plant C by both roots and microbes.

The typical pattern for gross photosynthesis at Willow Creek based on several years of eddy covariance measurements has been a parabolic curve peaking in June–July (Cook et al., 2004; Desai et al., 2005). This pattern mirrored our estimates of R_h/R_{tot} based on surface flux rates, suggesting that heterotrophic relative contributions reached a minimum when plant growth peaked. When we used an isotopic-mixing approach to partitioning, however, it suggested that heterotrophic contributions continued to remain low until the fall. A possible explanation of this discrepancy is that microorganisms in the intact plots switched during the growing season to substrates such as root exudates and new root litter that were more depleted in ^{14}C than the substrates initially available following spring thaw. The CO_2 respired from intact plots in late summer may have been produced by microbes but carried the $\Delta^{14}\text{C}$ signature of new roots. If microbes in intact plots switched to newly available substrates, then the trenched plot would no longer provide a good measure of heterotrophic $\Delta^{14}\text{C}$ for mixing-model partitioning.

Hopkins et al. (2013) have also shown that ^{14}C abundance in root respiration declines over the course of the growing season. While we measured root respiration at only a single time point and did not explicitly assess root respiration seasonal variability, the analysis by Hopkins et al. suggests that the root ^{14}C end-member is non-static through time. Their findings support our observation that soil respiration $\Delta^{14}\text{CO}_2$ declined in the presence of roots, and that more recent photosynthates tended to dominate respiration as the growing season passes.

We initially found that $\Delta^{14}\text{C}$ of surface flux from intact plots correlated with soil moisture; however, supporting analyses did not indicate a clear cause-and-effect relationship. We had expected that moisture might alter ^{14}C by changing vertical partitioning of soil respiration sources. We expected seasonal soil drying might cause shallow soils to become less active, due to water stress, and deep, seasonally saturated soils to become more active, due to improved oxygenation. This expectation was not substantiated, however, by the vertical partitioning analysis. Although we calculated that the percentage of CO_2 produced in the top 8 cm varied seasonally between 40–80%, we did not find a significant correlation with moisture, unless we included observations from the trenched plot. Observations from the trenched plot tended to have high leverage on regression analyses, because they grouped at the wet end of the soil moisture spectrum and at the high abundance end of the $\Delta^{14}\text{C}$ spectrum.

This points to the general challenge of parsing-out environmental drivers in soil respiration analyses. Because moisture in the trenched plot remained high through the summer, we could not assess the impacts of soil moisture in the absence of root inputs. Conversely, because root inputs covaried with moisture in the intact plots, it was also not entirely possible to assess the impacts of changing plant C allocation, independent of soil moisture changes.

In fact, one possibility is that estimates of heterotrophic soil respiration contributions (R_h/R_{tot}) based on bulk surface flux rates are overestimated during late summer, because of higher soil moisture levels in the trenched plot than in the intact plot. This could partially explain why isotopic partitioning estimates diverged from the bulk flux estimates. If microbial contributions were over-estimated in the late summer, however, this does not provide a satisfying explanation for the low $\Delta^{14}\text{CO}_2$ abundances respired from intact plots into the fall, as trees entered winter dormancy. The effects of moisture and changing C inputs may overprint one another, with late summer drought suppressing microbial respiration, and increasing contributions of new C both explaining the decline in $\Delta^{14}\text{CO}_2$ from intact plots from spring into fall.

4.2 In situ versus in vitro heterotrophic $^{14}\text{CO}_2$

The variation we observed in $^{14}\text{CO}_2$ respiration from the trenched plot indicated that the “active” C pool utilized by microbes is dynamic through time, varying at least 20%. Although the factors driving this variation could not be entirely discerned from this study (i.e., we did not find significant correlations between $\Delta^{14}\text{C}$ from the trenched plot and temperature or moisture), we had indirect evidence that microbes responded readily to changes in substrate availability.

We showed that $\Delta^{14}\text{CO}_2$ from soil incubations decreased with depth, reflecting the $\Delta^{14}\text{C}$ of bulk soil, whereas in situ CO_2 was modern through the soil profile. This discrepancy suggests that microbes at depth in the field were not consuming soil carbon from depth, but rather modern substrates that may have come from decaying roots (which were mostly picked out of the incubated soil cores), or from dissolved carbon transported from the shallow subsurface. Other field studies have previously noted modern $^{14}\text{CO}_2$ in soil air at depth (Gaudinski et al., 2000; Hirsch et al., 2003); however, previous studies were unable to rule-out root respiration as a source of this CO_2 . Because our trenching treatment cut off live roots, we were able to show that microbial activity can also produce modern CO_2 at depth in intact soil columns. Advective transport of substrates from the soil surface has been shown to create infillings of modern organic matter that serve as an important component of the “active” microbial C pool at depth in other ecosystems (Marin-Spiotta et al., 2011). Future work at Willow Creek that examines $\Delta^{14}\text{C}$ of dissolved organic carbon could help determine whether the source of modern carbon at depth is root inputs or surface carbon that is translocated.

4.3 Utility and limitations of $^{14}\text{CO}_2$ for understanding soil metabolism

The large seasonal range in soil-respired $\Delta^{14}\text{CO}_2$ found in this study points to exciting possibilities for using ^{14}C as a sensitive indicator of changing soil metabolism. Based on our findings and recent analyses by Hopkins et al. (2013), which show that root respiration from several forest sites becomes more similar to the atmosphere in ^{14}C content over the course of the growing season, we believe one of the more pronounced signals that can be detected using $\Delta^{14}\text{CO}_2$ measurements is the relative contributions of current photosynthates. A persistent challenge, however, is detecting the amount and type of C respired by soil microbes. At Willow Creek, it appears that recent photosynthates are an important substrate for microbial respiration, but in systems with large pools of old soil C, summer microbial activity may utilize much older C as well (Hartley et al., 2012).

Going forward, our study and others suggest more complexity involved in partitioning root and microbial respiration with $^{14}\text{CO}_2$ than was previously appreciated, as both end-members appear to be highly dynamic. We have several recommendations for others studying soil $^{14}\text{CO}_2$.

Use caution in extrapolating laboratory incubations to field conditions. Using laboratory incubations as an approximation for heterotrophic activity could compound, rather than simplify, interpretation of respired CO_2 sources. Laboratory incubations are useful for comparisons between disturbed soil cores, and within the context of understanding soil organic matter dynamics they can be used to assess the turnover time of the “active” C pool, or the pool that is most readily destabilized by microbial activity. Within the context of understanding in situ microbial activity, however, it becomes important to consider the more complete spectrum of microbial associations, including not only soil organic matter associations but also close associations with intact roots (Kuzakov, 2006). For deep soils in particular, in situ microbial respiration is likely much more impacted by root-derived C, and younger in terms of ^{14}C age, than is represented by soil incubations.

Consider an alternative scheme for partitioning sources of soil respiration. Partitioning soil respiration into root and microbial sources has been a persistent challenge for many years. Using ^{14}C as a tracer (Schoor and Trumbore, 2006), or a combination of ^{14}C and ^{13}C (Hicks Pries et al., 2013) are both approaches that have been used to isotopically partition root and microbial end-members. Such measurements usually depend on one-time measurements of the root and microbial end-members, because the sampling process is destructive, and ^{14}C measurements are costly. However, in light of the finding that root and microbial end-members may vary through time with inputs of new photosynthates, an alternative approach should be considered that focuses instead on partitioning respiration into present-year and older C stores. Such partitioning could be done without any destructive sam-

pling or extrapolation from incubations, and may be equally useful for studies that seek to examine coupling between above- and below-ground activity. Instead of measuring root and microbial end-members, a very early-season measurement of respired $\Delta^{14}\text{CO}_2$ could be used to represent the baseline condition, or the end-member for C sources from previous years, and atmospheric CO_2 could be measured as the end-member for new photosynthates. Repeated measurements through the growing season of respired $\Delta^{14}\text{CO}_2$ could be partitioned into present year and previous C sources using a two end-member mixing model. Such an approach may not be appropriate in all ecosystems, for example, if summer root inputs stimulate priming of old soil C pools (Hartley et al., 2012).

Dynamic models are a useful complement to static, steady-state models for interpreting soil gas data. In studies where deep soil C dynamics are of interest, analyses that go beyond directly measured values of surface flux $^{14}\text{CO}_2$ or soil air $^{14}\text{CO}_2$ to calculating flux and production profiles can also reveal useful insights about underlying sources of CO_2 that contribute to surface emissions. The steady-state Fickian models that are often used to calculate production profiles (e.g., Eqs. 7–9) are useful for this purpose but can have very large uncertainties, particularly if steady-state assumptions are violated. Dynamic models, like the Nickerson and Risk model demonstrated here, provide a useful alternative to constrain production profiles, and are also useful for investigating $^{14}\text{CO}_2$ responses to dynamic changes in soil environment.

Measure soil respiration $^{14}\text{CO}_2$ at the beginning, middle, and end of the growing season. For researchers primarily interested in an average growing season $\Delta^{14}\text{C}$ respiration value, this study corroborated previous work suggesting that seasonal variation in respired $^{14}\text{CO}_2$ is substantial (Hicks Pries et al., 2013; Hirsch et al., 2003; Hopkins et al., 2013; Schoor and Trumbore, 2006). At a minimum, sampling time points at the beginning, middle, and end of the growing season are ideal to capture the seasonal progression of new C additions.

5 Conclusions

By examining soil $^{14}\text{CO}_2$ with high vertical and temporal resolution we showed that respired $^{14}\text{CO}_2$ is strongly influenced by recently assimilated carbon; however, we could not fully resolve the mechanisms underlying low levels of $\Delta^{14}\text{C}$ late in the growing season and the correlation between $\Delta^{14}\text{C}$ and soil moisture. Our results indicated that heterotrophic $\Delta^{14}\text{C}$ is dynamic and sensitive to immediate substrate availability, and that experimental manipulations to isolate heterotrophic and autotrophic activity can substantially impact estimates of heterotrophic $\Delta^{14}\text{C}$. Inputs of new photosynthates over the growing season, which have been shown to decrease the ^{14}C content of root respiration (Hopkins et al.,

2013), may also lead to decreases in the ^{14}C content of microbial respiration. Studies that make use of ^{14}C measurements for examining disturbance or climatic change impacts should be interpreted with an understanding that respired ^{14}C can fluctuate seasonally by 40%, and that this variability may reflect not only changes in root contributions, but possibly root impacts on $\Delta^{14}\text{C}$ of heterotrophic respiration as well.

Acknowledgements. Field assistance was provided by J. Thom (UW) and D. Baumann (USGS), and laboratory assistance was provided by P. Zermefio and L. Larson (LLNL). This work was performed under the auspices of the US Department of Energy by Lawrence Livermore National Laboratory under contract DE-AC52-07NA27344, with support from Lawrence Livermore National Laboratory (LDRD 11-ERD-053) and the Wisconsin Focus on Energy Environmental and Economic Research and Development (EERD) grant# 10-06. LLNL-JRNL-637140.

Edited by: J.-A. Subke

References

- Albanito, F., McAllister, J. L., Cescatti, A., Smith, P., and Robinson, D.: Dual-chamber measurements of $\delta^{13}\text{C}$ of soil-respired CO_2 partitioned using a field-based three end-member model, *Soil Biol. Biochem.*, 47, 106–115, doi:10.1016/j.soilbio.2011.12.011, 2012.
- Andrews, A. E., Kofler, J. D., Trudeau, M. E., Williams, J. C., Neff, D. H., Masarie, K. A., Chao, D. Y., Kitzis, D. R., Novelli, P. C., Zhao, C. L., Dlugokencky, E. J., Lang, P. M., Crotwell, M. J., Fischer, M. L., Parker, M. J., Lee, J. T., Baumann, D. D., Desai, A. R., Stanier, C. O., de Wekker, S. F. J., Wolfe, D. E., Munger, J. W., and Tans, P. P.: CO_2 , CO and CH_4 measurements from the NOAA Earth System Research Laboratory's Tall Tower Greenhouse Gas Observing Network: instrumentation, uncertainty analysis and recommendations for future high-accuracy greenhouse gas monitoring efforts, *Atmos. Meas. Tech. Discuss.*, 6, 1461–1553, doi:10.5194/amtd-6-1461-2013, 2013.
- Bolstad, P. V., Davis, K. J., Martin, J. G., Cook, B. D., and Wang, W.: Component and whole-system respiration fluxes in northern deciduous forests, *Tree Physiol.*, 24, 493–504, 2004.
- Cerling, T. E., Solomon, D. K., Quade, J., and Bowman, J. R.: On the isotopic composition of carbon in soil carbon dioxide, *Geochim. Cosmochim. Ac.*, 55, 3403–3405, doi:10.1016/0016-7037(91)90498-T, 1991.
- Cisneros-Dozal, L. M., Trumbore, S. E., and Hanson, P. J.: Partitioning sources of soil-respired CO_2 and their seasonal variation using a unique radiocarbon tracer, *Glob. Change Biol.*, 12, 194–204, doi:10.1111/j.1365-2486.2005.001061.x, 2006.
- Cook, B. D., Davis, K., Wang, W., Desai, A. R., Berger, B. W., Teclaw, R. M., Martin, J. G., Bolstad, P. V., Bakwin, P. S., Yi, C., and Heilman, W.: Carbon exchange and venting anomalies in an upland deciduous forest in northern Wisconsin, USA, *Agr. Forest Meteorol.*, 126, 271–295, 2004.
- Czimczik, C. I., Trumbore, S. E., Carbone, M. S., and Winston, G. C.: Changing sources of soil respiration with time since fire in a boreal forest, *Glob. Change Biol.*, 12, 957–971, doi:10.1111/j.1365-2486.2006.01107.x, 2006.
- Davidson, E. A., Savage, K. E., Trumbore, S. E., and Borken, W.: Vertical partitioning of CO_2 production within a temperate forest soil, *Glob. Change Biol.*, 12, 944–956, doi:10.1111/j.1365-2486.2005.01142.x, 2006.
- Desai, A. R., Bolstad, P. V., Cook, B. D., Davis, K. J., and Carey, E. V.: Comparing net ecosystem exchange of carbon dioxide between an old-growth and mature forest in the upper Midwest, USA, *Agr. Forest Meteorol.*, 128, 33–55, 2005.
- Ewing, S. A., Sanderman, J., Baisden, W. T., Wang, Y., and Amundson, R.: Role of large-scale soil structure in organic carbon turnover: Evidence from California grassland soils, *J. Geophys. Res.*, 111, G03012, doi:10.1029/2006JG000174, 2006.
- Gaudinski, J. B., Trumbore, S. E., Davidson, E. A., and Zheng, S.: Soil carbon cycling in a temperate forest: radiocarbon-based estimates of residence times, sequestration rates and partitioning of fluxes, *Biogeochemistry*, 51, 33–69, 2000.
- Graven, H. D., Guilderson, T. P., and Keeling, R. F.: Observations of radiocarbon in CO_2 at La Jolla, California, USA 1992–2007: Analysis of the long-term trend, *J. Geophys. Res.-Atmos.*, 117, D02302, doi:10.1029/2011jd016533, 2012.
- Hahn, V., Höglberg, P., and Buchmann, N.: ^{14}C – a tool for separation of autotrophic and heterotrophic soil respiration, *Glob. Change Biol.*, 12, 972–982, doi:10.1111/j.1365-2486.2006.001143.x, 2006.
- Hartley, I. P., Garnett, M. H., Sommerkorn, M., Hopkins, D. W., Fletcher, B. J., Sloan, V. L., Phoenix, G. K., and Wookey, P. A.: A potential loss of carbon associated with greater plant growth in the European Arctic, *Nature Clim. Change*, 2, 875–879, doi:10.1038/nclimate1575, 2012.
- Hicks Pries, C. E., Schuur, E. A. G., and Crummer, K. G.: Thawing permafrost increases old soil and autotrophic respiration in tundra: Partitioning ecosystem respiration using $\delta^{13}\text{C}$ and $\delta^{14}\text{C}$, *Glob. Change Biol.*, 19, 649–661, 2013.
- Hirsch, A. I., Trumbore, S. E., and Goulden, M. L.: Direct measurement of the deep soil respiration accompanying seasonal thawing of a boreal forest soil, *J. Geophys. Res.*, 108, 8221, doi:10.1029/2001JD000921, 2003.
- Hopkins, F., Gonzalez-Meler, M. A., Flower, C. E., Lynch, D. J., Czimczik, C., Tang, J., and Subke, J.-A.: Ecosystem-level controls on root-rhizosphere respiration, *New Phytol.*, 199, 339–351, doi:10.1111/nph.12271, 2013.
- Kuzyakov, Y.: Sources of CO_2 efflux from soil and review of partitioning methods, *Soil Biol. Biochem.*, 38, 425–448, doi:10.1016/j.soilbio.2005.08.020, 2006.
- Lavoie, M., Owens, J., and Risk, D.: A new method for real-time monitoring of soil CO_2 efflux, *Methods Ecol. Evol.*, 3, 889–897, doi:10.1111/j.2041-210X.2012.00214.x, 2012.
- Marin-Spiotta, E., Chadwick, O. A., Kramer, M., and Carbone, M. S.: Carbon delivery to deep mineral horizons in Hawaiian rain forest soils, *J. Geophys. Res.*, 116, G03011, doi:10.1029/2010JG001587, 2011.
- Martin, J. G. and Bolstad, P. V.: Annual soil respiration in broadleaf forests of northern Wisconsin: influence of moisture and site biological, chemical, and physical characteristics, *Biogeochemistry*, 73, 149–182, 2005.

- Midwood, A. J. and Millard, P.: Challenges in measuring the $\delta^{13}\text{C}$ of the soil surface CO_2 efflux, *Rapid Commun. Mass Sp.*, 25, 232–242, doi:10.1002/rcm.4857, 2011.
- Moldrup, P., Olesen, T., Yoshikawa, S., Komatsu, T., and Rolston, D. E.: Three-porosity model for predicting the gas diffusion coefficient in undisturbed soil, *Soil Sci. Soc. Am. J.*, 68, 750–759, 2004.
- Nickerson, N. and Risk, D.: A numerical evaluation of chamber methodologies used in measuring the $\delta^{13}\text{C}$ of soil respiration, *Rapid Commun. Mass Spectrom.*, 23, 2802–2810, 2009a.
- Nickerson, N. and Risk, D.: Physical controls on the isotopic composition of soil-respired CO_2 , *J. Geophys. Res.*, 114, G01013, doi:10.1029/2008JG000766, 2009b.
- Nickerson, N., Egan, J., and Risk, D.: Iso-FD: A novel method for measuring the isotopic signature of surface flux, *Soil Biol. Biochem.*, 62, 99–106, 2013.
- Nickerson, N., Egan, J. and Risk, D.: Subsurface Approaches for Measuring Soil CO_2 Isotopic Flux: Theory and Application, *J. Geophys. Res.-Biogeosci.*, doi:10.1029/2013JG002508, in review, 2013.
- Phillips, C. L., Kluber, L. A., Martin, J. P., Caldwell, B. A., and Bond, B. J.: Contributions of ectomycorrhizal fungal mats to forest soil respiration, *Biogeosciences*, 9, 2099–2110, doi:10.5194/bg-9-2099-2012, 2012.
- Phillips, D. L. and Gregg, J. W.: Uncertainty of source partitioning using stable isotopes, *Oecologia*, 127, 171–179, 2001.
- Pingintha, N., Leclerc, M. Y., Beasley, J. P. J., Zhang, G., and Senthong, C.: Assessment of the soil CO_2 gradient method for soil CO_2 efflux measurements: comparison of six models in the calculation of the relative gas diffusion coefficient, *Tellus B*, 62, 47–58, 2010.
- Risk, D., Nickerson, N., Creelman, C., McArthur, G., and Owens, J.: Forced Diffusion soil flux: A new technique for continuous monitoring of soil gas efflux, *Agr. Forest Meteorol.*, 151, 1622–1631, doi:10.1016/j.agrformet.2011.06.020, 2011.
- Risk, D., McArthur, G., Nickerson, N., Phillips, C. L., Hart, C., Egan, J., and Lavoie, M.: Bulk and isotopic characterization of biogenic CO_2 sources and variability in the Weyburn injection area, *Int. J. Greenh. Gas Con.*, 16, S263–S275, doi:10.1016/j.ijggc.2013.02.024, 2013.
- Schrumpf, M., Kaiser, K., Guggenberger, G., Persson, T., Kögel-Knabner, I., and Schulze, E.-D.: Storage and stability of organic carbon in soils as related to depth, occlusion within aggregates, and attachment to minerals, *Biogeosciences*, 10, 1675–1691, doi:10.5194/bg-10-1675-2013, 2013.
- Schuur, E. A. G. and Trumbore, S. E.: Partitioning sources of soil respiration in boreal spruce forest using radiocarbon, *Glob. Change Biol.*, 12, 165–176, doi:10.1111/j.1365-2486.2005.01066.x, 2006.
- Southon, J. R.: Are the fractionation corrections correct: Are the isotopic shifts for $^{14}\text{C}/^{12}\text{C}$ ratios in physical processes and chemical reactions really twice those for $^{13}\text{C}/^{12}\text{C}$?, *Radiocarbon*, 53, 691–704, 2011.
- Stuiver, M. and Polach, H. A.: Discussion: Reporting of ^{14}C data, *Radiocarbon*, 19, 355–363, 1977.
- Torn, M. S., Lapenis, A. G., Timofeev, A., Fischer, M. L., Babikov, B. V., and Harden, J. W.: Organic carbon and carbon isotopes in modern and 100-year-old-soil archives of the Russian steppe, *Glob. Change Biol.*, 8, 941–953, doi:10.1046/j.1365-2486.2002.00477.x, 2002.
- Trumbore, S. E.: Age of soil organic matter and soil respiration: radiocarbon constraints on belowground C dynamics, *Ecol. Appl.*, 10, 399–411, 2000.
- Turcu, V. E., Jones, S. B., and Or, D.: Continuous soil carbon dioxide and oxygen measurements and estimation of gradient-based gaseous flux, *Vadose Zone J.*, 4, 1161–1169, 2005.
- Vogel, J. S., Southon, J. R., Nelson, D. E., and Brown, T. A.: Performance of catalytically condensed carbon for use in accelerator mass-spectrometry, *Nucl. Instrum. Methods*, B5, 289–293, 1984.